Magnetic ordering and ergodicity of the spin system in the $Cu_2Te_2O_5X_2$ family of quantum magnets

Z. Jagličić,[1] S. El Shawish,[2] A. Jeromen,[1] A. Bilušić,[3] A. Smontara,[3] Z. Trontelj,[1] J. Bonča,[2] J. Dolinšek,[2] and H. Berger[4]
[1]*Institute of Mathematics, Physics and Mechanics, University of Ljubljana, Jadranska 19, SI-1000 Ljubljana, Slovenia*
[2]*J. Stefan Institute, University of Ljubljana, Jamova 39, SI-1000 Ljubljana, Slovenia*
[3]*Institute of Physics, Bijenička 45, HR-10000 Zagreb, Croatia*
[4]*Institut de Physique de la Matière Complexe, EPFL, CH-1015 Lausanne, Switzerland*
(Received 26 April 2005; published 6 June 2006)

We present an experimental and theoretical study of the magnetically frustrated spin system in pure and substitutionally disordered compounds from the $Cu_2Te_2O_5X_2$ family of quantum magnets. Experimental magnetic susceptibilities and specific heats were analyzed simultaneously using models of (i) isolated tetrahedra of four antiferromagnetically coupled Cu^{2+} spins and (ii) coupled tetrahedra within one-dimensional chains, in both cases involving mean-field coupling to other chains. The results show that $Cu_2Te_2O_5X_2$ compounds are true three-dimensional systems of coupled spins. Susceptibility results are consistent with the existence of a singlet-triplet gap, whereas specific heat analysis shows that the singlet-triplet gap is filled with dense singlet-like excitations that contribute to finite specific heat at temperatures far below the singlet-triplet gap, but do not contribute to a magnetic response of the system. Furthermore, measured specific heat data show excessive entropy when compared to the numerical results based on a pure spin system, which we attribute to the presence of phonons. Though Cu^{2+} spins are arranged in a geometrically frustrated tetrahedral antiferromagnetic configuration and spin correlation length ξ extends beyond the single tetrahedral cluster dimension, $Cu_2Te_2O_5X_2$ compounds do not exhibit ergodicity breaking at low temperatures, in contrast to the related geometrically frustrated *kagomé* and pyrochlore antiferromagnets.

DOI: 10.1103/PhysRevB.73.214408 PACS number(s): 75.50.Lk, 75.30.−m

I. INTRODUCTION

In a magnetically frustrated system, the interaction between spins is such that no configuration can simultaneously satisfy all the bonds and minimize the energy at the same time.[1] Classical examples are canonical spin glasses (SGs) [dilute magnetic alloys of a noble metal host (Cu, Ag, Au) and a magnetic impurity (Fe, Mn)], where the interaction between spins is the conduction-electron-mediated Ruderman-Kittel-Kasuya-Yosida (RKKY) exchange interaction. This interaction oscillates in space and can be either ferromagnetic (FM) or antiferromagnetic (AFM), depending on the distance between spins. Combined with randomness (the spins must be positioned randomly in the sample), the RKKY interaction results in frustration. The free-energy landscape of a frustrated spin system is highly degenerate with a distribution of barriers between different metastable states, resulting in broken ergodicity below a spin freezing temperature T_f (i.e., the spin system cannot reach a thermodynamic equilibrium state on any accessible experimental time scale). Typical broken-ergodicity phenomena are: (i) a large difference between field-cooled (fc) and zero-field-cooled (zfc) magnetic susceptibilities below T_f in small magnetic fields, (ii) the zfc susceptibility exhibits a frequency-dependent cusp associated with a frequency-dependent freezing temperature $T_f(\omega)$, (iii) there exists an ergodicity-breaking line in the magnetic field-temperature (H-T) phase diagram (the de Almeida–Thouless line), (iv) the third-order nonlinear susceptibility χ_3 shows a sharp anomaly in the vicinity of T_f, and (v) there exist slow relaxation (aging) effects in the dc thermoremanent magnetization with time constants longer than any experimentally accessible time scale. At T_f, the spin correlation length ξ becomes very large (ξ^3 is the volume within which the spins develop correlations), so that all the spins in principle participate in the collective SG state. The spin systems involving frustration and randomness are known as "site-disordered" SGs.

It was discovered later that magnetically frustrated phases with similar broken-ergodicity properties also develop in pure (i.e., site-ordered) systems[2–6] without quenched disorder. These are geometrically frustrated antiferromagnets with *kagomé* and pyrochlore lattices, where triangular or tetrahedral distribution of nearest-neighbor AFM-coupled spins frustrates an ordered periodic system. The important difference to the site-disordered SGs is the short correlation length ξ usually encountered in geometrically frustrated AFMs, where ξ is already nonzero at relatively high temperatures (compared to T_f) and does not increase significantly with decreasing temperature. In the geometrically frustrated *kagomé* AFM $(H_3O)Fe_3(SO_4)_2(OH)_6$, short AFM correlations with $\xi \approx 1.9$ nm were reported,[6] and a similar ξ value was determined also in the pyrochlore system[2] $Tb_2Mo_2O_7$. Even shorter $\xi \approx 1$ nm was reported for another kind of geometrically frustrated pure systems, the icosahedral Ho-Mg-Zn and Tb-Mg-Cd quasicrystals,[7,8] where rare-earth spins are placed on an ordered quasiperiodic lattice. The short ξ values of the order 1 nm demonstrate that only near-neighbor spins or small cluster entities develop magnetic correlations. What really changes upon cooling is the characteristic time scale of the fluctuating moments, which slow down and exhibit a dramatic freezing below T_f, so that broken ergodicity remains a distinctive property of geometrically frustrated spin systems.

Recently, much experimental and theoretical effort has been put into the investigation of low-dimensional quantum

 ©2006 The American Physical Society

spin systems,[9] where reduced dimensionality in combination with frustration is considered to lead to unconventional ground states, interesting magnetic phase diagrams, and spin dynamics. The reduced dimensionality and frustration increase quantum fluctuations and the conventional picture of a long-range ordered Néel ground state breaks down. Unlike classical spin systems, characterized by some kind of low-temperature magnetic long-range order, quantum systems may reveal just a short-range magnetically ordered ground state, known as the spin-liquid state.[10] This spin-liquid state is characterized by finite (usually short) zero-temperature correlation length ξ and by the opening of a spin gap in the excitation spectrum.[10,11] Prominent examples are the frustrated and dimerized spin-1/2 chain, represented by the low-temperature phase of $CuGeO_3$, and the two-dimensional (2D) Shastry-Sutherland lattice with orthogonally arranged spin dimers and a frustrating interdimer coupling, realized[12] in $SrCu_2(BO_3)_2$. The spin-1/2 pyrochlore lattice deserves special attention, as it is believed to have very short correlation length and a singlet-triplet gap, eventually filled with low-lying singlet states.[13] It was suggested that a one-dimensional (1D) array of coupled tetrahedra with spins in an AFM configuration can be regarded as a 1D analog of the pyrochlore lattice.[13] The physical realization of such a system was reported to occur in the copper tellurates $Cu_2Te_2O_5X_2$ (X=Cl,Br),[14,15] where Cu^{2+} (S-1/2) spin tetrahedra form chains along the c-axis direction, making these systems convenient to study the interplay between the built-in frustration within the tetrahedra and magnetic coupling between them in a low-D quantum spin system. While there exist several experimental studies of magnetic ordering in the $Cu_2Te_2O_5X_2$ by measuring magnetic susceptibility,[14–16] specific heat,[15] Raman,[17] and infrared[18] spectra, neutron diffraction,[19] and thermal conductivity,[16] we are not aware of any systematic study of the interplay between frustration and ergodicity in low-D quantum spin systems that would allow comparison to the related geometrically frustrated AFMs and site-disordered SGs. Here we present a theoretical and experimental study of these effects in the $Cu_2Te_2O_5X_2$ family of quantum magnets, both pure and substitutionally disordered.

II. STRUCTURAL DETAILS AND FRUSTRATION

Pure $Cu_2Te_2O_5Cl_2$ and $Cu_2Te_2O_5Br_2$ possess intrinsic frustration of geometrical origin due to AFM-coupled Cu^{2+} spins within tetrahedra, which makes these systems resembling geometrically frustrated pure AFMs of a *kagomé* and pyrochlore type. As randomness is expected to amplify the frustration effect, we included in the study also substitutionally disordered $Cu_2Te_2O_5ClBr$, $Cu_2Te_2O_5Cl_{1.5}Br_{0.5}$, $Cu_2(Te_{1.8}Sb_{0.2})O_5Cl_2$, and $(Cu_{1.99}Co_{0.01})Te_2O_5Cl_2$ that contain certain degree of random topological disorder.

Frustration in the $Cu_2Te_2O_5X_2$ system should be intimately related to its structural details. Each copper atom is coordinated to three oxygen atoms and one chlorine or bromine atom creating a somewhat distorted square-planar CuO_3X coordination.[14] Four square planes are arranged in a way that Cu atoms form a distorted tetrahedron with two longer and four shorter Cu-Cu bonds. According to this, one expects two different exchange integrals, J_1 and J_2, between the Cu^{2+} spins of a given tetrahedral cluster. The Cu^{2+} tetrahedra align to tubes or chains along the c direction, which are separated along the a and b directions by different Te-O coordinations. The tellurium lone pairs point into large voids in the structure where they interact with the chlorine or bromine atoms. Coupling between the Cu^{2+} tetrahedral clusters is of crucial importance for the nature of the magnetic ground state. In the original work[14] it was reported that magnetic susceptibility of the $Cu_2Te_2O_5Cl_2$ and $Cu_2Te_2O_5Br_2$ is well reproduced by assuming that the systems are a collection of independent Cu^{2+} tetrahedra. In that case, frustration should be due to intratetrahedral AFM couplings of spins, hence of purely geometrical origin. It was reported later that significant intertetrahedral coupling J_c, comparable to the intratetrahedral J_1 and J_2, should be present in order to explain unusual magnetic ordering and longitudinal magnon[17] observed by Raman spectra, and incommensurate AFM order[19] observed by neutron diffraction in the $Cu_2Te_2O_5X_2$ compounds. The intertetrahedral couplings increase the range of spin interactions and make these systems more similar to the geometrically frustrated *kagomé* and pyrochlore AFMs.

Substitution of elements in the $Cu_2Te_2O_5X_2$ structure should add further to the frustration effect. The a and c lattice parameters of the Cl-compound are reduced by 3 and 1%, respectively, with respect to the Br-compound, so that the unit cell volume is reduced by 7%. Consqeuently, random $Cl \rightarrow Br$ substitution should lead to random variation of the interatomic distances, so that the exchange integrals may become distributed. A similar effect is expected to occur from substitution at other sites, e.g., $Cu \rightarrow Co$ and $Te \rightarrow Sb$. The $Cu \rightarrow Co$ substitution of coppers within the Cu^{2+} tetrahedra (the atoms that actually carry the spin) is in fact expected to yield the largest effect.

III. THEORETICAL MODEL AND METHOD

To get a theoretical insight into the magnetic ordering of $Cu_2Te_2O_5X_2$, we consider a model system built up from interacting tetrahedral clusters of S=1/2 spins forming a 1D chain along the z direction, with additional couplings to the neighboring chains treated within the mean-field approximation (MFA).[17,20] The Hamiltonian can be divided into

$$\mathcal{H} = \mathcal{H}_{chain} + \mathcal{H}_{MFA}, \tag{1}$$

where the first term represents the interaction of spins within the chain

$$\begin{aligned}\mathcal{H}_{chain} = {} & J_1 \sum_j (\mathbf{S}_{j,1}\cdot\mathbf{S}_{j,3} + \mathbf{S}_{j,2}\cdot\mathbf{S}_{j,4}) \\ & + J_2 \sum_j (\mathbf{S}_{j,1}\cdot\mathbf{S}_{j,2} + \mathbf{S}_{j,2}\cdot\mathbf{S}_{j,3} + \mathbf{S}_{j,3}\cdot\mathbf{S}_{j,4} + \mathbf{S}_{j,4}\cdot\mathbf{S}_{j,1}) \\ & + J_3 \sum_j (\mathbf{S}_{j,2}\cdot\mathbf{S}_{j+1,3} + \mathbf{S}_{j,4}\cdot\mathbf{S}_{j+1,1}) \\ & + J_4 \sum_j (\mathbf{S}_{j,2}\cdot\mathbf{S}_{j+1,1} + \mathbf{S}_{j,4}\cdot\mathbf{S}_{j+1,3}).\end{aligned} \tag{2}$$

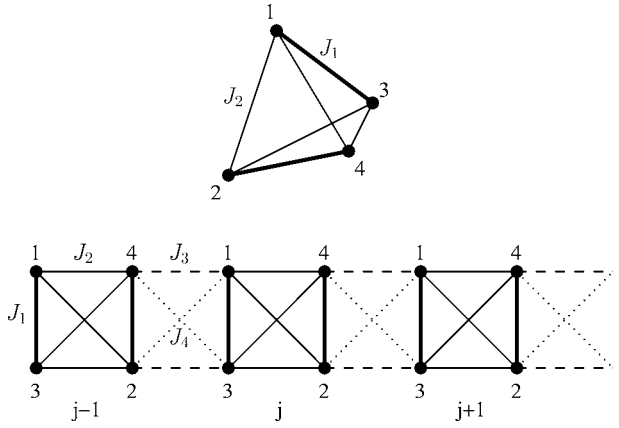

FIG. 1. Schematic representation of the coupling constants J_1 and J_2 within a single tetrahedron (top) and chain of tetrahedra (bottom), depicting the coupling constants J_3 and J_4 as well.

We label each tetrahedron by Latin indices j and assume periodic boundary conditions (PBC) along the chain. A schematic representation of different coupling constants is depicted in Fig. 1. J_1 and J_2 represent the intratetrahedral couplings, whereas J_3 and J_4 are the intertetrahedral couplings within the chain.

The coupling between neighboring chains is given in mean field as

$$\mathcal{H}_{MFA} = -2J_c M_z(T) \sum_j (S^z_{j,1} - S^z_{j,2} + S^z_{j,3} - S^z_{j,4}) + NJ_c M_z^2(T), \tag{3}$$

where $M_z(T)$ is the order parameter (the staggered magnetization)

$$M_z(T) = \frac{1}{N}\left\langle \sum_j S^z_{j,1} - S^z_{j,2} + S^z_{j,3} - S^z_{j,4} \right\rangle, \tag{4}$$

and N is the total number of spins. M_z enforces an ordered state, where the spins within pairs 1–3 and 2–4 are parallel, however spin alignment between pairs is antiparallel. This ordering takes full advantage of the J_1 interaction at the expense of J_2. For large enough J_c, the system orders at temperatures below the Néel temperature, $T < T_N$.

Our model Hamiltonian of Eqs. (1)–(4) is different from that used in previous works[17,20] from the point of view that it distinguishes between intratetrahedral couplings (J_1 and J_2), intertetrahedral couplings within a 1D chain (J_3 and J_4) and interchain coupling J_c, whereas earlier works have treated in mean field all the neighboring tetrahedra (those on the same chain and those on the neighboring chains). We are thus distinguishing between the "zero-D" case of isolated tetrahedra ($J_3 = J_4 = J_c = 0$), a 1D case of isolated chains ($J_c = 0$), and a full 3D case with all couplings different from zero. Complicated already enough, our model does not include substitutional effects.

In the following we present numerical results for $N=4$ (isolated tetrahedra on the chain with no PBC) and $N=16$ (a chain of four tetrahedra with PBC), including in both cases mean-field coupling to the neighboring chains. We calculate the temperature dependence of the magnetic susceptibility, χ, and the specific-heat contribution from spin degrees of freedom, c, according to

$$\chi = \frac{1}{N}\frac{\langle S^z_{tot}{}^2 \rangle}{T} \tag{5}$$

and

$$c = T\frac{\partial s}{\partial T} = \frac{1}{N}\frac{\partial \langle \mathcal{H} \rangle}{\partial T}, \tag{6}$$

where S^z_{tot} denotes the z component of the total spin and s is the magnetic entropy per spin. In Eqs. (5) and (6) all the fundamental physical constants are set to unity. Thermodynamic averages $\langle \cdots \rangle$ for the $N=16$ case were calculated using the finite-temperature Lanczos method (FTLM),[21,22] whereas for $N=4$, a standard exact-diagonalization (ED) approach was found to be more appropriate. The calculation of the thermodynamic quantities χ and c is done self-consistently. In the first step, a rather arbitrary initial distribution $M_{z,0}(T)$ is used to fix the parameters in $\mathcal{H}_{MFA}$ and then using FTLM (or ED), the first approximation $M_{z,1}(T)$ is calculated based on the Hamiltonian Eqs. (1)–(4) along with χ and c from Eqs. (5) and (6). Proceeding this way, the result of the ith step, $M_{z,i}(T)$, is used as the initial distribution for the next iteration. After p such steps, when $M_{z,p}(T)$ has converged within a given accuracy ε, the procedure is stopped by setting $M_z(T) \equiv M_{z,p}(T)$. In practice, the number of iterations p strongly depends on temperature, having a maximum value of the order 30 at $T \approx T_N$ for $\varepsilon = 0.01$ and $N=16$. The iteration process may be shortened if the shape of $M_z(T)$ is roughly known and preset in the initial distribution $M_{z,0}(T)$.

IV. COMPARISON TO EXPERIMENT

All the investigated samples were monocrystals grown by chemical vapor transport technique, using $TeCl_4$ and $TeBr_4$ as transport agents, and the details of preparation are described elsewhere.[14,16] The study included four $Cu_2Te_2O_5(Cl_xBr_{1-x})_2$ compounds ($x=0$, 0.5, 0.75, and 1) and substituted $Cu_2(Te_{1.8}Sb_{0.2})O_5Cl_2$ and $(Cu_{1.99}Co_{0.01})Te_2O_5Cl_2$, where the Sb and Co concentrations are nominal.

The temperature-dependent magnetic susceptibility $\chi(T)$ was measured between 300 and 2 K in a field $H=100$ Oe, where the magnetization M is linear with H [actually we found that a linear $M(H)$ relation holds up to the highest measuring field of 5 T], so that we discuss $\chi = M/H$ in the following. A quantum design SQUID magnetometer was used. All samples were oriented with the c axis parallel to H. The experimental $\chi(T)$ curves are displayed in Fig. 2(a), whereas the low-temperature portions below 50 K are displayed on an expanded temperature scale in Fig. 2(b). All susceptibilities exhibit a maximum somewhere between 20 and 30 K. For the pure $Cu_2Te_2O_5Cl_2$ and $Cu_2Te_2O_5Br_2$ compounds, the maxima occur at $T_{max}=23$ and 30 K, respectively, in agreement with the literature data,[14–16] whereas the $\chi(T)$ maxima of the four substitutionally disordered samples

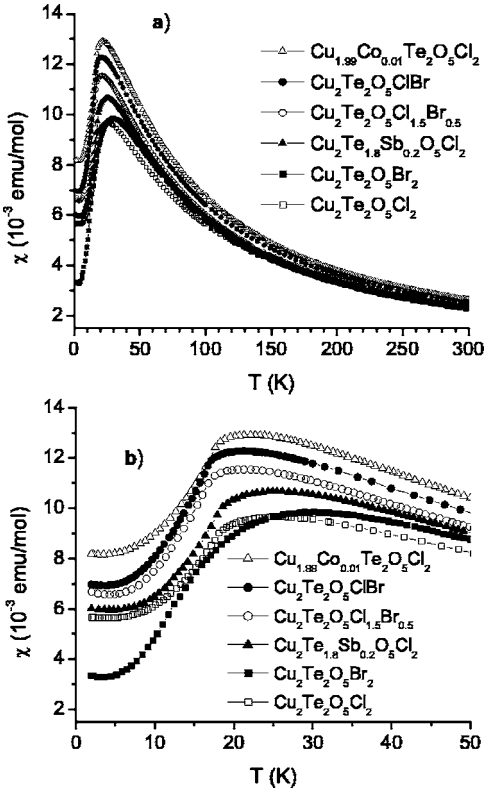

FIG. 2. (a) Magnetic susceptibilities of pure and substitutionally disordered single-crystalline samples from the $Cu_2Te_2O_5X_2$ family between 300 and 2 K in a field $H=100$ Oe. (b) The data below 50 K are shown on an expanded temperature scale.

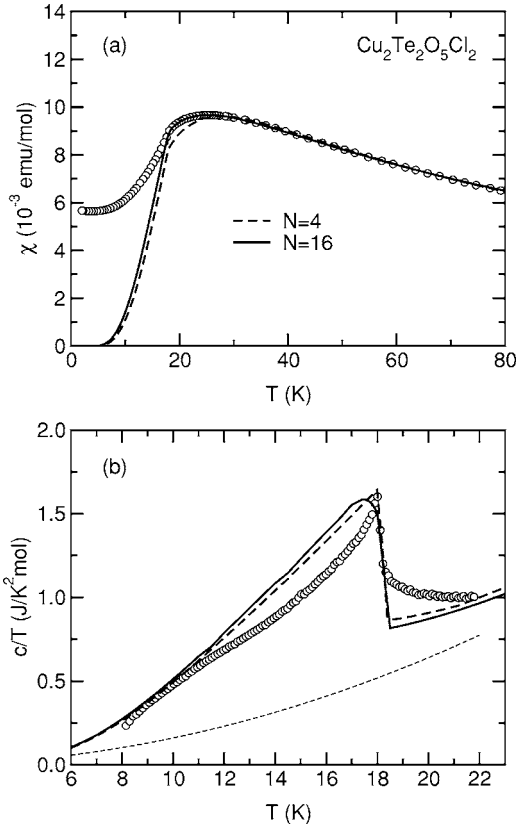

FIG. 3. (a) Magnetic susceptibility χ and (b) specific heat c/T of the $Cu_2Te_2O_5Cl_2$ compound. The $N=16$ (solid line) and $N=4$ (long-dashed line) numerical fits were made in absolute units of the experiment (see the text). The fit of the specific heat is a sum of magnetic and phononic contributions, $c/T=(c/T)_{mag}+(c/T)_{ph}$, where the phononic contribution is shown by a short-dashed line.

occur between 21 and 25 K. Another significant difference is the magnitude of the low-temperature saturation plateau $\chi(T\rightarrow 0)$. This plateau is the lowest for the two pure compounds and increases for the substitutionally disordered samples. This can be understood by considering the AFM configuration of spins in the ground state. In the substituted compounds, substitutional disorder acts to destroy local symmetry, resulting in reduced antiparallel spin compensation and higher residual $\chi(0)$ values as compared to the pure compounds. From this point of view, the substitution of magnetic coppers within the Cu^{2+} tetrahedra is expected to yield the largest effect. In Fig. 2(b) it is observed that this is indeed the case; the $(Cu_{1.99}Co_{0.01})Te_2O_5Cl_2$ sample exhibits the largest residual susceptibility.

The significant nonzero residual susceptibility prevents us from getting reliable information on the existence of a spin gap Δ in the excitation spectrum from the low-temperature analysis, so that fitting of the high-temperature portion of χ only makes sense. The susceptibility fits alone are, however, not very sensitive to the choice of the fit parameters, as several combinations of the exchange integrals give comparable fits. For that reason we conducted additional measurements of the specific heat c by the standard calorimetric method and performed simultaneous fitting of both χ and c/T, using the same set of parameters. Specific heats of the investigated samples exhibit a well-pronounced mean-field-like anomaly at the temperature T_N, where magnetic ordering sets in, so that the mean-field coupling constant J_c can be reliably determined from the shape and position of the anomaly. Moreover, the model parameters were extracted from the fits using *absolute* units of the experiment (taking into account fundamental physical constants, we obtain relations $\chi[\text{emu/mol}]=0.7503[\text{emu K/mol}]g^2\langle S^{z^2}_{tot}\rangle/NT[\text{K}]$ and $c[J/\text{mol K}]=16.63[J/\text{mol K}]N^{-1}(\partial\langle\mathcal{H}\rangle/\partial T)$, where g is the Landé factor and the fact that there are two coppers in the $Cu_2Te_2O_5X_2$ formula unit has been taken into account).

The predictions of the microscopic model were compared to the measured data of the four $Cu_2Te_2O_5(Cl_xBr_{1-x})_2$ compounds. In Figs. 3–6 the comparison of the experimental susceptibilities χ and the specific heats c/T with the numerical results for the isolated-tetrahedra ($N=4$) system are displayed. Since calculations for the chain of tetrahedra represent a much greater numerical effort, we present additional $N=16$ results only for the two pure ($x=0$ and 1) compounds. For the susceptibility χ, the agreement between the theory and experiment in the temperature range $T>T_N$ seems rather good, independent of the compound. Even g factors that have been varied in order to obtain optimal fits fall within the physically relevant regime (e.g., for the pure Cl compound we obtain $g_4=2.03$ and $g_{16}=2.08$, whereas $g=2.08$ was reported in Ref. 14. For the Br compound we get $g_4=2.07$ and $g_{16}=2.15$, as compared to $g=2.15$ of Ref. 14). Disagreement with the experimental data below the transition to the or-

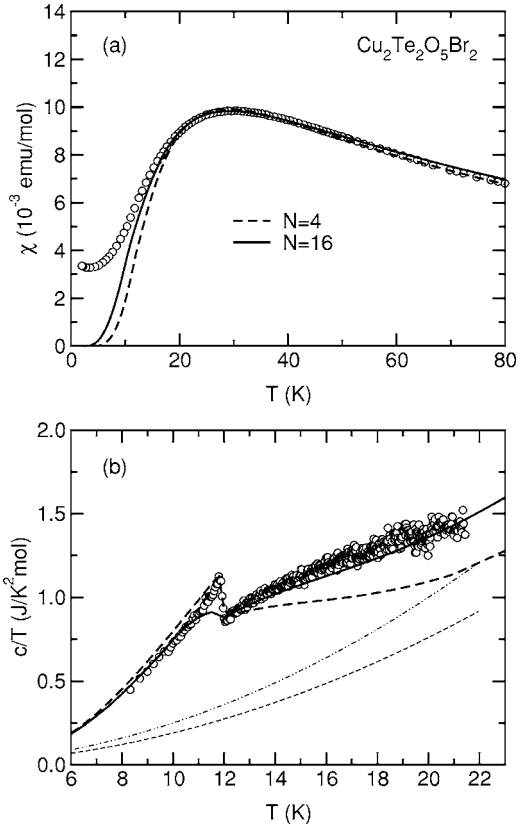

FIG. 4. (a) Magnetic susceptibility χ and (b) specific heat c/T of the $Cu_2Te_2O_5Br_2$ compound with the $N=16$ (solid line) and $N=4$ (long-dashed line) numerical fits. The phononic contribution to the specific heat for the $N=4$ case is shown by a short-dashed line, whereas for the $N=16$ case it given by the dash-dotted line.

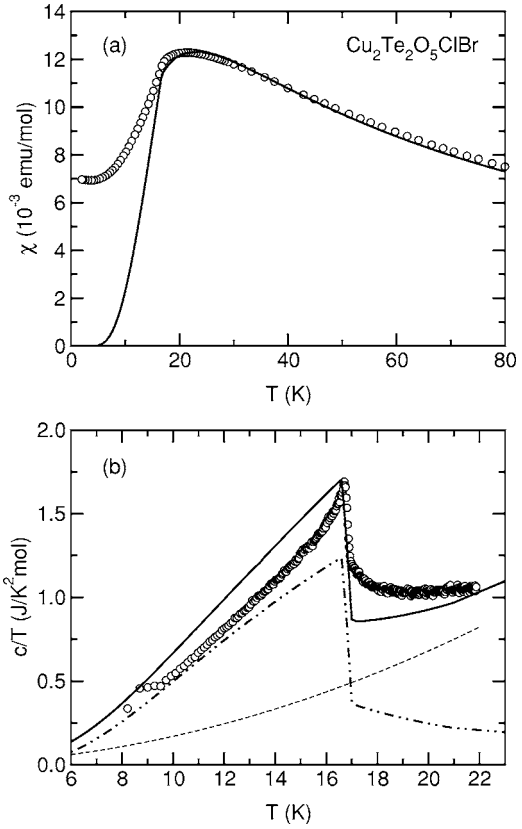

FIG. 5. (a) Magnetic susceptibility χ and (b) specific heat c/T of the $Cu_2Te_2O_5ClBr$ compound with the $N=4$ (solid line) fits. The phononic contribution to the specific heat, $(c/T)_{ph}$, is shown by a short-dashed line, whereas the magnetic contribution, $(c/T)_{mag}$, is shown by a dash-dotted line.

dered state, $T<T_N$, is attributed in part to the crystalline imperfections (finite quality of the samples) and in part to the substitution-induced incomplete antiparallel spin compensation that both yield nonzero residual susceptibility $\chi(0)$. We should also stress that we have computed only the longitudinal susceptibility χ_{zz}. Below the transition to the ordered state, the spin rotation invariance within MFA is broken, so that one expects $\chi_{zz}\neq\chi_{xx}$. Combining longitudinal and transverse part of the susceptibility tensor might lead to better agreement with the experiment for $T<T_N$.

Comparing the experimental and theoretical specific heat c/T data in absolute units we find, in contrast to the results of χ, that numerical c/T due to spin degrees of freedom [in the following referred to as $(c/T)_{mag}$] deviates significantly from the experimental data even at $T>T_N$ for all four substances. Numerical data systematically fall below the experimental data, suggesting that in the real material there is excessive entropy generated by other degrees of freedom, not taken into account by a pure spin model of Eq. (6). Adding a phononlike term, $(c/T)_{ph}=\beta T^2$, brings our numerical results much closer to the experimental data. The presence of phonons in the $Cu_2Te_2O_5X_2$ is supported by the thermal conductivity $\kappa(T)$ measurements,[16] where a maximum in $\kappa(T)$ at low temperature, typical of phonon thermal transport, was observed.

In Fig. 3(a) we present the experimental susceptibility χ of the pure $Cu_2Te_2O_5Cl_2$ with the numerical $N=4$ (long-dash) and $N=16$ (solid line) fits. The resulting fit parameters are listed in Table I. We observe that the addition of the intertetrahedral couplings within the chain, J_3 and J_4, slightly improves the fit around the transition to the ordered state, i.e., in the range $T\gtrsim T_N$. Consequently, the optimal values of J_1, J_2, J_c, and g have also changed. In the $N=4$ case, the couplings $J_1=37.0$ K, $J_2=45.0$ K, and $J_c=31.2$ K are of comparable size, whereas in the $N=16$ case, the intratetrahedron couplings $J_1=38.3$ K and $J_2=42.5$ K are significantly larger than the intertetrahedron ($J_3=8.5$ K and $J_4=17.0$ K) and the MFA ($J_c=22.1$ K) couplings. The experimental c/T data and the $c/T=(c/T)_{mag}+(c/T)_{ph}$ fits are displayed in Fig. 3(b). The anomaly in c/T at the transition to the ordered state is observed at $T_N=18$ K, in agreement with the literature data.[15] The c/T fits of the $N=4$ (long-dash) and $N=16$ (solid line) cases are reasonable, exhibiting only an insignificant difference, predominantly due to small numerical errors generated by the FTLM method. Most importantly, calculation on a larger system does not raise the magnitude of $(c/T)_{mag}$ that remains well below the experimental data. The phonon contribution $(c/T)_{ph}=\beta T^2$ is shown as a short-dashed line, where the same value of the fit parameter $\beta_4=\beta_{16}=16$ mJ/K^4 mol was used in both fits.

The same analysis was performed for the other pure compound, $Cu_2Te_2O_5Br_2$, and the results are displayed in Fig. 4. The anomaly in c/T is observed here at $T_N=11.6$ K. The N

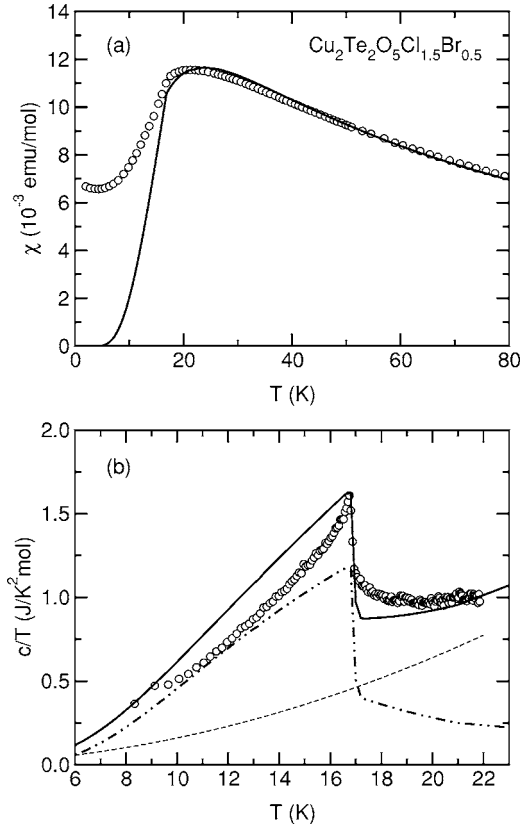

FIG. 6. (a) Magnetic susceptibility χ and (b) specific heat c/T of the $Cu_2Te_2O_5Cl_{1.5}Br_{0.5}$ compound with the $N=4$ (solid line) fits. The phononic contribution to the specific heat, $(c/T)_{ph}$, is shown by a short-dashed line, whereas the magnetic contribution, $(c/T)_{mag}$, is shown by a dash-dotted line.

$=16$ fit [solid line in Fig. 4(a)] again reproduces the susceptibility χ to a somewhat lower temperature than the $N=4$ fit (long-dashed line) and the exchange integrals (Table I) are of the same magnitude and relative proportion (J_1 and J_2 are significantly larger than J_3, J_4, and J_c) as for the Cl compound. The specific heat is displayed in Fig. 4(b). Apart from a lack of a sharp transition peak in c/T at $T=T_N$ on a $N=16$ system, the agreement with the experimental data is better than in the Cl case. We should note that in order to obtain a good fit, a different $\beta_{16}=25$ mJ/K^4 mol value was used than in the $N=4$ case (where $\beta_4=19$ mJ/K^4 mol).

The $N=4$ analyses of the substitutionally disordered $Cu_2Te_2O_5ClBr$ and $Cu_2Te_2O_5Cl_{1.5}Br_{0.5}$ are displayed in Figs. 5 and 6, respectively. For the $Cu_2Te_2O_5ClBr$, the c/T anomaly is observed at $T_N=16.5$ K [Fig. 5(b)], whereas it occurs at about the same temperature, $T_N=16.8$ K, in the $Cu_2Te_2O_5Cl_{1.5}Br_{0.5}$ [Fig. 6(b)]. The c/T fits, showing separately the magnetic and phononic contributions, are reasonable. The same applies to the χ fits and the fit parameters are collected in Table I. We observe that J_1 and J_c couplings are practically the same, whereas J_2 is significantly larger.

The above simultaneous analysis of the experimental χ and c/T data yields the following conclusions. On the one hand, the maximum in the susceptibility and the significant decrease of χ below are consistent with a finite gap between a singlet ground state and the lowest excited triplet state. This behavior is also characteristic of spin liquids. On the other hand, specific heat shows temperature dependence that is similar to ordered AFMs and is not compatible with an exponentially thermally activated behavior expected for a system with a gap. The chain of the coupled tetrahedra model ($N=16$ case) gives a better description than the isolated tetrahedra on the chain ($N=4$). The intratetrahedral couplings J_1 and J_2 are about a factor two larger than the intertetrahedral J_3, J_4, and the mean-field J_c couplings, so that the intratetrahedral interactions are dominant. Under the conditions $J_1<J_2$ and $J_2/2<J_1$ (that are met in all investigated compounds), the ground state and the first excited state of isolated tetrahedra are spin singlets, so that one would expect a finite gap in the excitation spectrum for negligible J_3, J_4, and J_c, as compared to J_1 and J_2. However, our numerical calculations show that moderate intertetrahedral couplings create a band of low-lying singlets, which fill the singlet-triplet gap and contribute to finite specific heat at temperatures far below the singlet-triplet gap, whereas they do not contribute to the magnetic response of the system. Low-lying dense singletlike excitations are thus the reason for the apparent discrepancy between the susceptibility that is typical of a spin-gap system and the specific heat that does not show activated behavior characteristic of a spin gap at low temperature, but resembles regular AFMs. The investigated $Cu_2Te_2O_5(Cl_xBr_{1-x})_2$ quantum magnets thus appear to be true 3D systems of coupled spins, where the intercluster interactions are strong enough to suppress the intracluster singlet formation. Consequently, the spin correlation length ξ extends significantly beyond the single Cu^{2+} tetrahedral cluster dimension.

TABLE I. Fit parameters (see text) obtained from simultaneous analysis of the magnetic susceptibility χ and specific heat c/T.

	N	J_1 [K]	J_2 [K]	J_3 [K]	J_4 [K]	J_c [K]	g	β [mJ/K^4 mol]
$Cu_2Te_2O_5Cl_2$	4	37.0	45.0			31.2	2.03	16
	16	38.3	42.5	8.5	17.0	22.1	2.08	16
$Cu_2Te_2O_5Br_2$	4	31.5	46.0			20.2	2.07	19
	16	27.3	45.4	9.08	18.2	8.6	2.15	25
$Cu_2Te_2O_5ClBr$	4	26.0	37.0			25.6	2.07	17
$Cu_2Te_2O_5Cl_{1.5}Br_{0.5}$	4	22.0	37.0			23.9	2.01	16

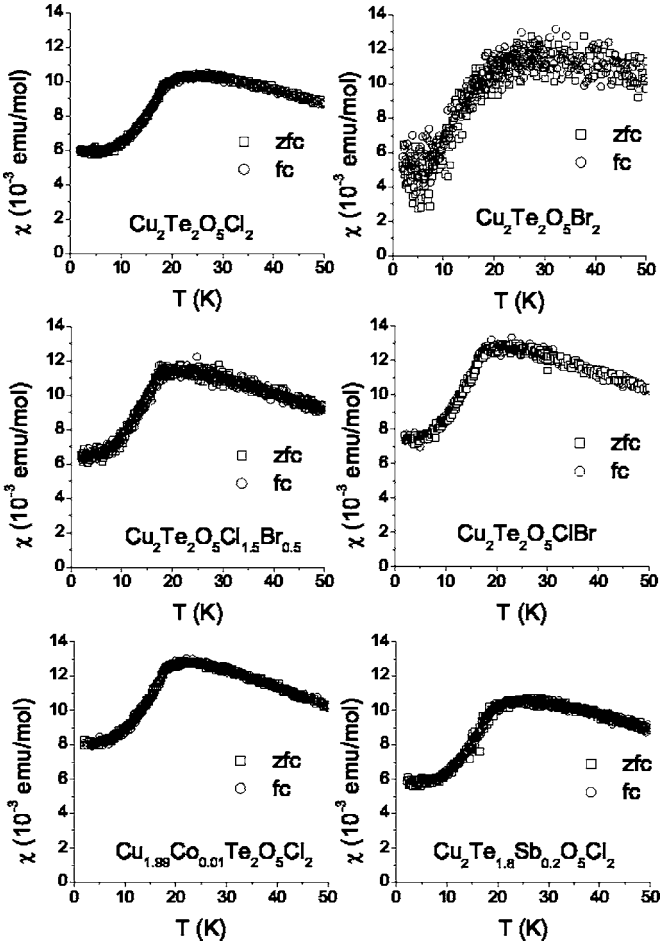

FIG. 7. zfc and fc susceptibilities between 50 and 2 K in a dc field $H=1$ Oe.

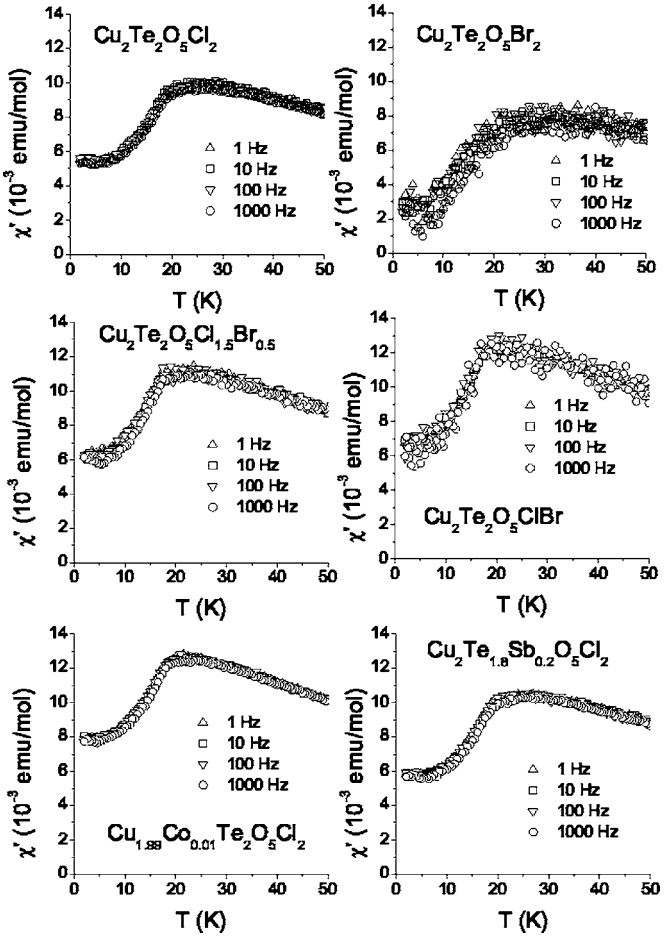

FIG. 8. ac magnetic susceptibilities χ' between 50 and 2 K measured in an ac field of amplitude $H_{ac}=6.5$ Oe and frequencies between 1 and 1000 Hz.

V. ERGODICITY

Having demonstrated that $Cu_2Te_2O_5X_2$ compounds are 3D frustrated spin systems, it is interesting to consider ergodicity breaking in such a system, in comparison to the related geometrically frustrated AFMs and site-disordered SGs. As discussed above, one of the commonly observed phenomena in magnetically frustrated systems is the zfc-fc magnetization splitting below the freezing temperature T_f, indicating the temperature below which the ergodicity of the spin system is broken on a given experimental time scale. Our zfc-fc experiments were performed in a low dc magnetic field of $H=1$ Oe only, in order that the external field has negligible influence on the spontaneous magnetic ordering in the samples. One complete zfc-fc cycle involved cooling the sample in zero field to 2 K, switching on the field and slowly heating to 50 K followed by a slow cooling in the field back to 2 K. The zfc-fc susceptibilities of all samples are displayed in Fig. 7. The results are rather astonishing—no zfc-fc splitting is observed down to 2 K for any of the six samples. Here it is important to stress that the temperature 2 K is already far below the magnetic ordering temperatures of the investigated samples. As no zfc-fc splitting occurs down to the lowest measured temperature, the ergodicity of the spin system is not broken down to 2 K in any of the investigated pure and substitutionally disordered systems.

Another check of the ergodicity breaking is the measurement of the ac susceptibility χ' in the fields of different frequency. We applied ac fields with logarithmically spaced frequency of 1, 10, 100, and 1000 Hz in the same temperature interval (50 to 2 K). The results are displayed in Fig. 8. We again observe consistently for all samples that there is no frequency dependence of χ' down to 2 K. This is another proof that the ergodicity of the investigated crystals is not broken in the investigated temperature interval.

Slow relaxation of the thermoremanent magnetization (TRM) is considered as another prominent manifestation of broken ergodicity.[23–26] In a TRM experiment, the sample is cooled in a low magnetic field from a temperature high above T_f to a "measuring" temperature $T_m < T_f$, where the cooling is stopped for a "waiting time" t_w, so that the spin system is let to approach an equilibrium state in the field H. After t_w, the field is suddenly cut off to zero, which results in an almost instantaneous decay of the reversible part of the magnetization, followed by a slow decay of the irreversible part (TRM) of the magnetization (that can amount up to 10% of the total magnetization[24–26]). The slow TRM decay is a consequence of high barriers in the free energy landscape of a frustrated system, which should be surmounted in order

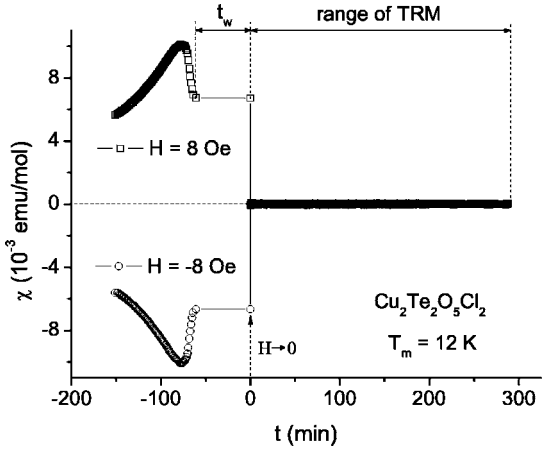

FIG. 9. Thermoremanent magnetization decay experiment (see the text) performed on the $Cu_2Te_2O_5Cl_2$ sample. The origin of the time scale ($t=0$) coincides with the moment of the field cutoff. Identical result (zero TRM) was found for all samples at any measuring temperature T_m down to 2 K.

that the spin system can approach the equilibrium state in zero field from the initial $H \neq 0$ state. Our TRM experiments were performed by cooling to various T_m's starting at 50 K and letting the system equilibrate for $t_w=60$ min before the field cutoff. Two symmetric field-cooled experiments in $H=\pm 8$ Oe were performed each time. The TRM experiment for the $Cu_2Te_2O_5Cl_2$ sample performed at $T_m=12$ K is displayed in Fig. 9, where it is observed that no TRM exists after the field cutoff. The same result was obtained for all other samples, choosing any T_m down to 2 K. In view of the fact that the dc susceptibilities displayed in Fig. 7 show no zfc-fc splitting (the TRM is just the difference between the fc and zfc susceptibilities) down to 2 K, this result is not surprising and the TRM decay curves of other samples are not shown.

VI. CONCLUSIONS

Experiments and theoretical analysis of the magnetic susceptibility χ and specific heat c/T demonstrate that $Cu_2Te_2O_5X_2$ compounds are true 3D systems of coupled spins. Susceptibility results are consistent with the existence of a singlet-triplet gap. Specific heat data show that the singlet-triplet gap is filled with dense singletlike excitations that contribute to finite specific heat at temperatures far below the singlet-triplet gap, whereas they do not contribute to the magnetic response of the system. Consequently, the temperature dependence of specific heat is similar to that of ordered AFMs. Furthermore, measured specific heat data show excessive entropy when compared to the numerical results based on a pure spin system, which we attribute to the presence of phonons. Since Cu^{2+} spins are arranged in a geometrically frustrated tetrahedral AFM configuration and spin correlation length ξ extends beyond the single tetrahedral cluster dimension, $Cu_2Te_2O_5X_2$ resemble geometrically frustrated kagomé and pyrochlore AFMs. However, the observed absence of the zfc-fc magnetization splitting, the frequency-independent ac susceptibility, and zero TRM demonstrate that ergodicity of the investigated pure and substitutionally disordered $Cu_2Te_2O_5X_2$ compounds is not broken down to the lowest measuring temperature of 2 K, which is much below the reported temperatures of magnetic ordering in these systems. The macroscopic manifestation of frustration in the $Cu_2Te_2O_5X_2$ quantum magnets does not occur in the same way as in the frustrated SGs and AFMs, where it leads to freezing of the spin dynamics and ergodicity breaking at low temperatures.

ACKNOWLEDGMENTS

The sample preparation in Lausanne was supported by the NCCR research pool MaNEP of the Swiss NSF.

[1] See, e.g., K. Binder and A. P. Young, Rev. Mod. Phys. **58**, 801 (1986), and references therein.
[2] B. D. Gaulin, J. N. Reimers, T. E. Mason, J. E. Greedan, and Z. Tun, Phys. Rev. Lett. **69**, 3244 (1992).
[3] A. Lafond, A. Meerschaut, J. Rouxel, J. L. Tholence, and A. Solpice, Phys. Rev. B **52**, 1112 (1995).
[4] P. Schiffer, A. P. Ramirez, D. A. Huse, P. L. Gammel, U. Yaron, D. J. Bishop, and A. J. Valentino, Phys. Rev. Lett. **74**, 2379 (1995).
[5] M. J. P. Gringras, C. V. Stager, N. P. Raju, B. D. Gaulin, and J. E. Greedan, Phys. Rev. Lett. **78**, 947 (1997).
[6] A. S. Wills, V. Dupuis, E. Vincent, J. Hammann, and R. Calemczuk, Phys. Rev. B **62**, R9264 (2000).
[7] T. J. Sato, H. Takakura, A. P. Tsai, K. Shibata, K. Ohoyama, and K. H. Andersen, Phys. Rev. B **61**, 476 (2000).
[8] T. J. Sato, H. Takakura, J. Guo, A. P. Tsai, and K. Ohoyama, J. Alloys Compd. **342**, 365 (2002).
[9] See, e.g., *Magnetic Systems with Competing Interactions*, edited by H. T. Diep (World Scientific, Singapore, 1994).
[10] F. Mila, Eur. J. Phys. **21**, 499 (2000), and references therein.
[11] P. Lemmens, G. Guntherodt, and C. Gros, Phys. Rep. **375**, 1 (2003).
[12] S. Miyahara and K. Ueda, J. Phys.: Condens. Matter **15**, R327 (2003).
[13] M. Mambrini, J. Trébosc, and F. Mila, Phys. Rev. B **59**, 13806 (1999).
[14] M. Johnsson, K. W. Törnroos, F. Mila, and P. Millet, Chem. Mater. **12**, 2853 (2000).
[15] P. Lemmens, K.-Y. Choi, E. E. Kaul, Ch. Geibel, K. Becker, W. Brenig, R. Valenti, C. Gros, M. Johnsson, P. Millet, and F. Mila, Phys. Rev. Lett. **87**, 227201 (2001).
[16] M. Prester, A. Smontara, I. Živković, A. Biluši, D. Drobac, H. Berger, and F. Bussy, Phys. Rev. B **69**, 180401(R) (2004).
[17] C. Gros, P. Lemmens, M. Vojta, R. Valentí, K.-Y. Choi, H. Kageyama, Z. Hiroi, N. V. Mushnikov, T. Goto, M. Johnsson, and P. Millet, Phys. Rev. B **67**, 174405 (2003).

[18] A. Perucchi, L. Degiorgi, H. Berger, and P. Millet, Eur. Phys. J. B **38**, 65 (2004).
[19] O. Zaharko, A. Daoud-Aladine, S. Streule, J. Mesot, P.-J. Brown, and H. Berger, Phys. Rev. Lett. **93**, 217206 (2004).
[20] J. Jensen, P. Lemmens, and C. Gros, Europhys. Lett. **64**, 689 (2003).
[21] J. Jaklič and P. Prelovšek, Adv. Phys. **49**, 1 (2000); J. Jaklič and P. Prelovšek, Phys. Rev. Lett. **77**, 892 (1996).
[22] G. A. Jorge, R. Stern, M. Jaime, N. Harrison, J. Bonča, S. E. Shawish, C. D. Batista, H. A. Dabkowska, and B. D. Gaulin, Phys. Rev. B **71**, 092403 (2005).
[23] M. Lederman, R. Orbach, J. M. Hammann, M. Ocio, and E. Vincent, Phys. Rev. B **44**, 7403 (1991).
[24] D. Chu, G. G. Kenning, and R. Orbach, Philos. Mag. B **71**, 479 (1995).
[25] J. Dolinšek, Z. Jagličić, M. A. Chernikov, I. R. Fisher, and P. C. Canfield, Phys. Rev. B **64**, 224209 (2001).
[26] J. Dolinšek, Z. Jagličić, T. J. Sato, J. Q. Guo, and A. P. Tsai, J. Phys.: Condens. Matter **15**, 7981 (2003).